Scar and antiscar quantum effects in open chaotic systems

L. Kaplan*
Department of Physics and Society of Fellows, Harvard University, Cambridge, Massachusetts 02138
(Received 21 August 1998; revised manuscript received 3 February 1999)

We predict and numerically observe strong periodic orbit effects in the properties of weakly open quantum systems with a chaotic classical limit. Antiscars lead to a large number of exponentially narrow isolated resonances when the single-channel (or tunneling) opening is located on a short unstable orbit of the closed system; the probability to remain in the system at long times is thus exponentially enhanced over the random matrix theory prediction. The distribution of resonance widths and the probability to remain are quantitatively given in terms of only the stability matrix of the orbit on which the opening is placed. The long-time remaining probability density is nontrivially distributed over the available phase space; it can be enhanced or suppressed near orbits other than the one on which the lead is located, depending on the periods and classical actions of these other orbits. These effects of the short periodic orbits on quantum decay rates have no classical counterpart, and first appear on times scales much larger than the Heisenberg time of the system. All the predictions are quantitatively compared with numerical data. [S1063-651X(99)12805-8]

PACS number(s): 05.45.−a, 03.65.Sq

I. INTRODUCTION

A. Wave-function scarring

Wave-function scarring, the enhancement or suppression of quantum eigenstate intensity along an unstable orbit of the corresponding classical system, is a fascinating and generic property of quantum chaotic behavior. Along with dynamical localization, it is one of the striking ways in which a quantum system can show deviation from ergodicity at the single-channel level even though the classical dynamics is completely ergodic. Wave-function intensities near a short unstable periodic orbit follow a distribution far from that predicted by random matrix theory (RMT), with some wave-functions having much more intensity and other much less than would be predicted based on Gaussian random fluctuations. The phenomenon is at first glance paradoxical, because the long-time (and indeed stationary) quantum behavior retains a memory of the short-time classical motion, a memory that is completely absent in the long time *classical* dynamics of a chaotic system. Scarring has been observed experimentally in a wide variety of systems, including microwave cavities [1,2], semiconductor structures [3], and the hydrogen atom in a magnetic field [4,5].

A theory of scarring based on the linearized evolution of Gaussian wave packets was first provided in Ref. [6]; later theoretical work by Bogomolny [7] in coordinate space and Berry [8] in Wigner phase space followed. These made predictions about the average intensity on a classical periodic orbit of states in a given energy band; however, because of the energy smoothing involved, no predictions were possible about the statistical properties of individual peak heights in the local density of states. Subsequently, Agam and Fishman [9] developed the idea of detecting and quantifying scars by integrating wave-function intensity over tubes in phase space surrounding the periodic orbit. More recently a nonlinear theory was developed [10] which made it possible to predict the statistical properties of individual wave functions, in the semiclassical limit. A homoclinic orbit analysis showed that long-time return amplitude to the vicinity of a periodic orbit bore the imprint of the short-time linearized classical dynamics around the periodic orbit. This leads to a natural separation of scarring intensity into a classical short-time component and a random long-time component, as suggested already in Ref. [11].

In Ref. [12], predictions were made about the distribution of wave-function intensities on a periodic orbit and at a generic point in phase space. The full distribution of intensities, which includes samples taken over all of phase space, has a long tail (compared to the Porter-Thomas prediction of RMT), dominated by the effect of the least unstable periodic orbit. The functional form of this tail is given in the semiclassical (high-energy) limit very simply in terms of the stability exponent of this least unstable orbit, as long as an optimally oriented test basis is chosen. Furthermore, upon ensemble averaging a power-law intensity distribution tail is obtained, in sharp contrast with the exponential tail predicted by RMT. This result is also to be contrasted with the log-normal intensity distribution tail which obtains in diffusive systems [13,14]. Thus, although RMT is accepted as the zeroth-order approximation for both chaotic and disordered quantum systems (i.e., it is the dynamics-free baseline with which true system properties are to be compared), deviations from RMT predictions can be qualitatively different in the two cases, providing an impetus for the present research.

B. Chaotic scattering

The numerically tested quantitative predictions in Refs. [10,12] concerned the local densities of states in a closed system. Certain properties of open systems, such as resonance widths and conductances, may, however, be more amenable to experimental verification [15]. Much important theoretical work has been done on the problem of quantum chaotic scattering, mostly in the regime of a large number of open incoming and outgoing channels. This is a very natural limit to take, for example, in billiard (hard wall) systems with a fixed geometry, where the number of open channels

*Electronic address: kaplan@physics.harvard.edu

becomes large as the wavelength decreases. In this subsection we discuss a few of the established results in the scattering literature. We begin by mentioning particularly the important early work of Gaspard and Rice, who studied the classical, semiclassical, and quantum problem of a point particle scattering off three hard disks in a plane [16]. The metastable classical states there were observed to be fractal and chaotic, with chaos (as measured by the rate of KS entropy increase per unit time) inhibiting the rate of classical escape from the system. Interestingly, some of the quantum scattering resonances have lifetimes significantly longer than that of the longest-lived classical resonance. This enhancement of certain quantum lifetimes can be understood semiclassically as an interference effect, and indeed a semiclassical upper bound on possible quantum lifetimes was obtained using a symbolic code for the classical dynamics.

The three-disk model was also used by Eckhardt [17] in his analysis of the spectral form factor and its relation to delay times in an open system. In analogy with closed system behavior, the short-time quantum dynamics was found to be nonuniversal and governed by a few isolated unstable periodic orbits. At longer times, statistical interference between many classical trajectories takes over, and a classical escape law holds. Finally, at very long times, lifetimes of individual narrow quantum resonances dominate the rate of decay. [In the present work, transmission through very small openings is considered, so the resonances are always isolated and the bulk of the decay necessarily takes place in this long time individual-resonance regime.] We also note that in earlier work, Cvitanovic and Eckhardt [18] showed that the quantum resonances of a three-disk system can be accurately computed semiclassically, using cycle expansions which express the effects of long periodic orbits in terms of a few short classical trajectories.

Blumel and Smilansky [19] studied carefully the effect of irregular classical scattering on the quantum scattering matrix and its energy correlations, in the same limit of many open channels (i.e., strongly overlapping resonances). Semiclassical arguments were used to show that fluctuations with energy of the S matrix and cross section should be consistent with Ericson fluctuations, previously observed in the context of nuclear scattering. Ericson fluctuations are a direct consequence of RMT, and such fluctuations were indeed measured numerically, inside energy ranges (scaling as $\hbar^{-1}$) where the statistical semiclassical arguments are expected to work.

Doron, Smilansky, and Frenkel [20] studied chaotic scattering with application to electronic transport through mesoscopic devices as well as to the transmission of microwaves through junctions. Fluctuations in the transmission coefficient were again shown to be consistent with RMT predictions, and the dependence of transmission correlations on external parameters was examined. Connections were made with the time domain behavior of chaotic systems, and the effect of absorption was discussed. Jalabert, Baranger, and Stone [21] showed that ballistic chaotic conductors display universal conductance fluctuations (UCF's), the magnitude of the fluctuations being of order one channel and independent of the total number of channels transmitted. They pointed out that these (RMT-predicted) fluctuations arise from interference, and are not obtainable for a classical S matrix. The authors also noticed nonuniversal behavior arising from short trajectories through the device, i.e., those trajectories which are short compared to the classical mixing time of the system. The universal regime is expected to hold when the typical trajectory is trapped for many bounces (so that a statistical analysis of the transport is valid), and yet is short compared to the Heisenberg time (so that the resonances are wide and many of them overlap at any given energy). Of course, in the semiclassical limit of high energy or large system size, it is easy to satisfy simultaneously these two conditions.

Jung and Seligman [22] have analyzed carefully the important distinction that must be made between chaos in a Hamiltonian flow and chaos in the resulting classical scattering map. They have given several examples of chaotic scattering maps arising from integrable dynamics without topological chaos, and have studied the quantum mechanics of these unusual systems. The authors found that eigenphase statistics of the quantum S matrix depend primarily on the chaoticity of the scattering map, whereas basis-dependent quantities such as the distribution of matrix elements tend to follow RMT behavior only in the presence of topological chaos.

Finally, we mention the work of Borgonovi, Guarneri, Rebuzzini, and Shepelyansky [23], who have studied quantum transport fluctuations in the context of kicked chaotic maps, and specifically in modified versions of the quantum kicked rotor. They have again observed Ericson-like transmission fluctuations; the transmission probability is self-correlated on an energy scale related to the inverse time that the particle spends in the interaction region. In the diffusive regime, the amplitude of the UCF's ($\approx 2/15$) was found to be in good agreement with RMT expectations. The statistics of S matrix fluctuations were also numerically investigated, in various transport regimes. For ballistic transport, the fluctuating part of the S matrix agrees well with a Gaussian random model, but systematic deviations from RMT were observed once transport through the device became diffusive. In the diffusive (ohmic) regime, S matrix correlations also begin to deviate from a Lorentzian shape. Finally, in the quasi-one-dimensional localized regime, the distribution of transmission rates becomes log-normal, consistent with the prediction for an Anderson insulator.

The literature we have been discussing focuses almost exclusively on the regime of large classical openings, with many open channels and a strongly overlapping resonance structure. In that context, deviations from RMT that arise in the presence of disorder have also been considered [24]. In the present work, we focus on the opposite limit of small openings in a classically chaotic system, where the resonances are isolated and have a one-to-one correspondence with the eigenstates of a closed system. The isolated resonance regime appears in the presence of leads narrow compared to a wavelength, and more generally when tunneling is the source of coupling of a chaotic system to the outside world. [Numerical calculations are now in progress for a simple model where metastable states decay through tunneling out of a smooth potential well.] Much work has been done to analyze narrow openings within the context of RMT [25]. Here we address (going beyond the naive RMT approximation) the distribution of decay lifetimes in a leaky chaotic system, and the probability to remain in such a system [26] as a function of time and the location of the

''leak'' (open channel). The distribution in phase space of the remaining probability density at long times is considered, as well as the dependence of the probability to remain on where the particle was first ''injected'' into the system. These last two questions bring us into contact with wavefunction correlations and transport in chaotic systems, which (as we show) can be very different from RMT expectations where periodic orbits are involved. All the quantitative predictions which follow are tested numerically. A study of conductance properties in two-lead chaotic systems, including mean conductance, conductance fluctuations, distribution of peak heights, and peak correlations (and how all these depend on the placement of one or both leads in relation to the classical orbits) is forthcoming [27].

II. CLASSICAL AND QUANTUM WEAKLY OPEN CHAOTIC SYSTEMS

A. Classical behavior

We begin by considering a small opening in a classically chaotic system, which allows a particle to escape from the system. We will often use language suggesting that the ''opening'' is defined in position space, as it would often be, for example, in a mesoscopic experiment. However, the formalism considered here is much more general: all that is required is that the opening be localized in the classical *phase space*; escape routes that are defined exclusively in terms of position or momentum are special cases of this. A simple example of a momentum space opening is a potential barrier that allows particles to leave only if their momentum is directed almost normal to the wall [28]. An opening having the shape of a phase-space Gaussian naturally occurs when one considers tunneling out of a metastable chaotic well formed by a continuous potential [29].

Now we can imagine forming a mesh in classical phase space with each cell the size of the opening; because the classical dynamics (in the closed system) is chaotic, probability density starting in one such cell will soon be evenly distributed over all the available cells. The time for this to happen is logarithmic in the size of the opening w:

$$T_{\mathrm{mix}} \sim \frac{|\ln w|}{\overline{\lambda}}. \tag{1}$$

Here $\overline{\lambda}$ is the Lyapunov exponent of the classical dynamics (the mean rate of chaotic divergence of classical orbits), and the total size of phase space, in terms of which w must be measured, has been set to unity. On the other hand, the escape time from the system is inversely proportional to the leak size w, so a small value of w will cause complete mixing of the remaining probability to take place on a time scale much shorter than the scale on which probability is leaking out. One obvious consequence is that the probability to remain in the open classical system follows an exponential law. [Exponential classical decay depends on the chaotic (strongly mixing) nature of the classical system: in such systems the Frobenius-Perron operator has an *isolated* eigenvalue at 1. Nonexponential decay laws may obtain in integrable systems, even for an infinitesimal opening.] This behavior is, of course, independent of the position of the leak. Also, density is constantly redistributing itself, so that the remaining probability density remains evenly distributed on the scale of our mesh, except in a corridor of length scaling as $1/\overline{\lambda}$ leading forward in time from the position of the opening. Notice that the width of the corridor where the probability to remain is suppressed scales as the size of the opening. Thus, this corridor has no effect on the quantum behavior when the opening is small compared to $\hbar$. Finally, even if the initial probability is not evenly distributed over the entire phase space, the long-time behavior is unaffected (as long as the bulk of the probability is not initially placed in a corridor similar to the one described above, but leading *backwards* in time from the opening).

In contrast to these results, we will find in the quantum case that the probability to remain in the system at long times depends strongly on whether the opening is located on a classical (unstable) periodic orbit, even though the initial probability density is evenly distributed. Again, we see that long-time quantum behavior retains a better memory of short-time classical dynamics than does the long-time classical behavior. Also, we will see that given a leak placed on a periodic orbit, the remaining probability distribution at long times can be strongly affected not just on the periodic orbit itself, but also on the *other* short periodic orbits of the system. Enhancement or suppression can be observed depending on the energy range considered and on the classical actions of the orbits in question. Similarly, the probability to remain at long times will be affected if the original probability is injected on an unstable periodic orbit different from the one where the opening is located. All this is true even though the decay is taking place on a time scale much longer than any other time scale in the problem (the period of the short orbit, the mixing time, and also the Heisenberg time, i.e., $\hbar$ over the mean level spacing).

B. Quantum mechanics and RMT

Let the quantization of our classical system be given by an N-dimensional Hilbert space (N is the number of Planck-sized cells in the classical phase space), with dynamics in the closed system given by the Hamiltonian H_0. If the opening is very small (less than one open channel, so that the resonances are nonoverlapping), we can write an effective Hamiltonian for the open system

$$H = H_0 - i\frac{\Gamma}{2}|a\rangle\langle a|, \tag{2}$$

where $|a\rangle$ is a quantum channel associated with the opening, and Γ is the decay rate in that channel (taken to be small). $|a\rangle$ could be a Gaussian wavepacket enclosing the hole, or a position or momentum state. It is important to note here that the opening is small compared to $\hbar$ (less than half a wavelength if in position space). One can of course consider the effects of scarring on larger openings, or ones which are not thus localized to a single channel; these possibilities are considered towards the end of the present paper. We emphasize, however, that the phenomenon discussed here is already present in its full form for the tiniest single opening, without the complications that arise in the more general case.

For a small hole, the main effect of the opening on a wave function $|\Psi_n\rangle$ of the closed system is that it acquires a decay width proportional to the intensity of the wave function at the opening:

$$\Gamma_n = \Gamma |\langle \Psi_n | a \rangle|^2. \tag{3}$$

If the intensities $x_n \equiv N|\langle \Psi_n|a\rangle|^2$ follow a chi-squared distribution, as in RMT, we have probability $P(x) = (1/\sqrt{2\pi x})\exp(-x/2)$ for real overlaps $\langle \Psi_n|a\rangle$, and $P(x) = \exp(-x)$ for complex overlaps. Consider the complex case. Because mixing between the states of the closed system can be neglected in the small Γ regime, the total probability to remain in the system is given by a sum over these states

$$\begin{aligned} P_{\rm rem}(t) &= \frac{1}{N}\sum_{n=0}^{N-1} e^{-(x_n/N)\Gamma t} \\ &= \int_0^\infty dx P(x) e^{-x\Gamma t/N} \\ &= \int_0^\infty dx e^{-x} e^{-x\Gamma t/N} = \frac{1}{1+\Gamma t/N}. \end{aligned} \tag{4}$$

(Remember that N is the total number of states in the system; the classical decay rate is given by $\Gamma_{\rm cl} = \Gamma/N$ because only one channel has the possibility to decay.) We see that at short times ($t \ll \Gamma_{\rm cl}^{-1}$), the probability to remain in the system is $P_{\rm rem}(t) \approx 1 - \Gamma_{\rm cl} t$, as expected, while at long times we have the asymptotic behavior

$$P_{\rm rem}(t) \approx \frac{1}{\Gamma_{\rm cl} t}. \tag{5}$$

In the case of M independent weakly open channels, i.e.,

$$H = H_0 - i\sum_{i=0}^{M-1} \frac{\Gamma^{(i)}}{2} |a^{(i)}\rangle\langle a^{(i)}|, \tag{6}$$

the classical decay rate is given by

$$\Gamma_{\rm cl} = \frac{1}{N}\sum_{i=0}^{M-1} \Gamma^{(i)} \tag{7}$$

and the RMT probability to remain is

$$P(t) = \prod_{i=0}^{M-1} \frac{1}{1+\Gamma^{(i)} t/N}. \tag{8}$$

Taking $M \to \infty$ while keeping the total decay rate $\Gamma_{\rm cl}$ constant, exponential decay consistent with the classical prediction is obtained. On the other hand, fixing the number of channels M and taking $t \to \infty$, we observe the power-law behavior

$$P_{\rm rem}(t) = \frac{(N/t)^M}{\prod_{i=0}^{M-1} \Gamma^{(i)}}. \tag{9}$$

The case of real overlaps $\langle \Psi_n|a\rangle$ follows similarly: each real random overlap counts as half of a complex one, so there $P_{\rm rem}(t) \sim t^{-M/2}$. In the literature one often considers the distribution of delay times for scattering off of the system in question: there one must include the probability of populating a given resonance in the first place, which of course is proportional to Γ_n. This leads to an extra factor of t in the denominator, giving $P_{\rm delay}(t) \sim t^{-M-1}$ for complex overlaps and $P_{\rm delay}(t) \sim t^{-M/2-1}$ for real overlaps. In our case, we imagine the system to be populated first, before the lead is opened up, and thus no extra power of t is present.

III. EFFECT OF PERIODIC ORBITS

A. Probability to remain

We now go beyond RMT to consider the effect of real dynamics on the quantum probability to remain in a classically chaotic system. Take the escape channel $|a\rangle$ to be on or near an (unstable) periodic orbit of instability exponent λ. The smoothed local density of states at $|a\rangle$ is obtained by Fourier transforming its short-time autocorrelation function, which is easily obtained by linearizing the classical equations of motion near the unstable orbit [6,10,12]. Thus, for example, if the periodic orbit in question is a fixed point of a discrete time map, and $|a\rangle$ is a Gaussian wave packet optimally aligned along the stable and unstable manifolds of the orbit, then the short-time autocorrelation function (in the closed system) is given by

$$A_{\rm lin}(t) \equiv \langle a|a(t)\rangle = \frac{e^{-i\phi t}}{\sqrt{\cosh \lambda t}}. \tag{10}$$

Here $-\phi$ is a phase associated with one iteration of the orbit: it is given by the classical action in units of $\hbar$, plus a Maslov phase as appropriate. The subscript ''lin'' indicates that the expression is obtained within the linearized classical approximation; it is valid on time scales short compared to the mixing time $T_{\rm mix} \sim |\ln \hbar|/\lambda$.

A more general form of Eq. (10) applies for a nonoptimally oriented wave packet (e.g., a position state or momentum channel could be nonoptimal depending on the direction of the invariant manifolds at the periodic point), and also for a channel not exactly centered on a periodic point [27,30]. In particular, for a wave packet centered on the periodic orbit but not optimally oriented with respect to its invariant manifolds, the form above becomes

$$A_{\rm lin}(t) = \langle a|a(t)\rangle = \frac{e^{-i\phi t}}{\sqrt{\cosh \lambda t + iQ \sinh \lambda t}}. \tag{11}$$

In Eq. (11), Q is a nonoptimality parameter: in a coordinate system where the stable and unstable manifolds are orthogonal, Q is a function of the angle between the orientation of the phase-space Gaussian (at some fixed eccentricity) and either of these two directions. Alternatively, if the wave packet $|a\rangle$ is fixed to have a circular shape in phase space (i.e., to have equal and uncorrelated uncertainties in q and p), Q becomes a function of the nonorthogonality between the stable and unstable manifolds. In any case, as long as Q is not very large, the qualitative behavior is not much changed, and although analytic results are less easy to obtain for nonzero Q, quantitative predictions can be readily produced for comparison with any experimental or numerical data. The key point for our purposes here is that for a small

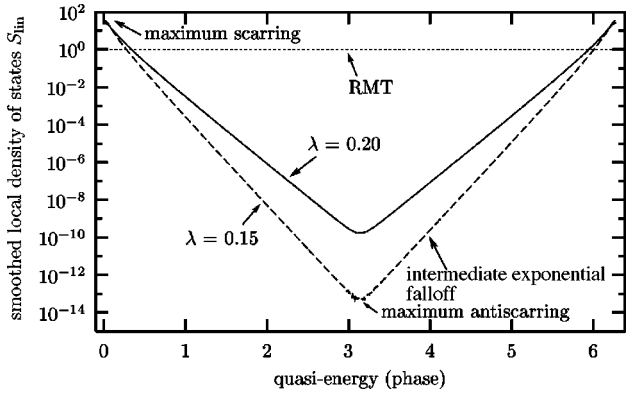

FIG. 1. Smoothed local densities of states $S_{\mathrm{lin}}(E)$ are plotted as a function of energy on a periodic orbit of instability exponent $\lambda = 0.20$ (solid curve) and on an orbit with $\lambda = 0.15$ (dashed curve). The mean resonance width for a lead placed on such a periodic orbit will be proportional to $S_{\mathrm{lin}}(E)$. We observe the peak at the EBK quantization energy $E=0$ [Eq. (16)] which scales as λ^{-1}, the exponential decay between $E=0$ and $E=\pi$ [Eq. (17)], and the minimum at the anti-EBK energy $E=\pi$, which is exponentially small in λ [Eq. (18)]. The RMT prediction $S_{\mathrm{lin}}(E)=1$, which is applicable away from any short periodic orbit, is plotted as a dotted line.

exponent λ, the autocorrelation function remains large for the first $O(\lambda^{-1})$ iterations of the orbit, and the local density of states has a short-time envelope

$$S_{\mathrm{lin}}(E) \equiv \sum_t e^{iEt} A_{\mathrm{lin}}(t) \tag{12}$$

of width scaling as λ and height scaling as λ^{-1} (also see Fig. 1 below).

Nonlinear recurrences on time scales beyond the mixing time (associated with orbits homoclinic to the original periodic orbit) lead to fluctuations multiplying this spectral envelope, eventually producing a line spectrum

$$S(E) = \sum_n |\langle \Psi_n | a \rangle|^2 \delta(E - E_n). \tag{13}$$

The line heights $x_n = N|\langle \Psi_n | a \rangle|^2$ are distributed in each energy region as a chi-squared distribution with mean $S_{\mathrm{lin}}(E)$ [12]:

$$P(x) = \frac{1}{S_{\mathrm{lin}}(E)} e^{-x/S_{\mathrm{lin}}(E)}. \tag{14}$$

Thus, the distribution of decay widths can be strongly energy dependent; in particular, the probability to remain in the system at long times is now given by

$$\begin{aligned} P_{\mathrm{rem}}(t) &= \int_0^\infty dx P(x) e^{-x\Gamma t/N} \\ &= \frac{1}{1 + S_{\mathrm{lin}}(E)\Gamma t/N} \\ &\to \frac{1}{S_{\mathrm{lin}}(E)} \frac{1}{\Gamma_{\mathrm{cl}} t} \end{aligned} \tag{15}$$

if initially only states with energy around E are populated.

The scarred states (those with energy close to satisfying the EBK quantization condition) have $S_{\mathrm{lin}}(E) > 1$ and thus decay much faster than the antiscarred states [11], which are far from satisfying EBK and thus have $S_{\mathrm{lin}}(E) < 1$. Let us examine more closely these two distinct energy regimes. Near the quantization energy $E = \phi$, the smoothed density of states $S_{\mathrm{lin}}(E)$ has its peak; its height scales inversely with λ for small λ [6]:

$$S_{\mathrm{lin}}(E = \phi) \approx c/\lambda, \tag{16}$$

where $c = 5.24$ is a numerical constant [12]. The width of this peak in $S_{\mathrm{lin}}(E)$ scales linearly with λ for small λ, and all of the anomalously enhanced wave-function intensities come from this energy region, as was observed and confirmed numerically in Ref. [12]. In the open system, these states produce an excess of large resonance decay widths and decay faster [by a factor of $O(\lambda^{-1})$] than would be predicted by RMT.

(We note that our presentation here is in the context of a discrete-time map; thus E is a dimensionless quasienergy that takes values in the interval $[0, 2\pi]$. For a real continuous-time system with a periodic orbit of period T_P, it is of course the quantity $ET_P/\hbar$ that must be compared with the dimensionless number λ. Also, the smoothed density of states will then have an infinite sequence of peaks, each centered on an energy satisfying the EBK quantization condition [10]. The ratio of each peak width to the spacing between peaks scales as λ. The infinite sequence of scarring peaks is modulated by a wide envelope associated with the energy width ΔE of the initial wave packet: in the semiclassical limit, this width is large compared to the spacing between peaks and small compared to the total energy. In the time domain, the scale ΔE is associated with the finite time $T_F \sim \hbar/\Delta E$ which the wave packet takes to traverse itself under free evolution each time that its center returns to the original position [10].)

Because our focus here is on the long-time behavior of weakly open systems, we are more interested in the (complementary) suppression of the smoothed local density of states far from the resonance energy. Again, we consider the strong scarring regime, where $\lambda \ll 1$: then the linear spectrum falls off exponentially far away from the peak

$$S_{\mathrm{lin}}(E) \approx \frac{2\pi}{\lambda} e^{-\pi |E - \phi|/2\lambda} \tag{17}$$

for $|E - \phi| \gg \lambda$. Within $O(\lambda)$ of the optimal antiscarring energy, $E = \phi + \pi$, the spectrum deviates from the exponential law and smoothly approaches the value

$$S_{\mathrm{lin}}(E = \phi + \pi) \approx \frac{4\pi}{\lambda} e^{-\pi^2/2\lambda} \tag{18}$$

at the minimum. The region within $O(\lambda)$ of $E = \phi + \pi$ is thus responsible for producing the smallest wave-function intensities, and the narrowest resonances in the corresponding open system. This excess of exponentially small decay rates is as dramatic a signature of the underlying classical behavior as the long wave-function intensity distribution tails found in [12]. As we will observe in the next section, the antiscarring effect on the long-time behavior of open systems

can be very striking even for moderate exponents λ (e.g., $\lambda \approx 1$), as long as the lead is optimally placed with respect to the periodic orbit.

Smoothed local densities of states $S_{\rm lin}(E)$ on periodic orbits of instability exponents $\lambda = 0.20$ (solid curve) and $\lambda = 0.15$ (dashed curve) are shown graphically in Fig. 1. The figure can be viewed as representing the average wavefunction intensity on the periodic orbit in a closed system as a function of energy, or the mean resonance width (in units of $\Gamma_{\rm cl}$) at that energy in the weakly open system. The phase $\phi = 0$ has been chosen so as to make $E = 0$ the EBK energy at which maximum scarring occurs [Eq. (16)]. A half-log scale is used to emphasize the exponential falloff in average resonance width between $E = 0$ and $E = \pi$ [Eq. (17)], and the minimum near the anti-EBK energy $E = \pi$ [Eq. (18)]. For reference, the smoothed local density of states in RMT (applicable when the lead is not in the vicinity of any short periodic orbit) is displayed as a dotted line in the figure.

We now consider the energy-averaged probability to remain in the open system: this will be the quantity studied in detail numerically in the next section, where the model system is a (nonenergy conserving) discrete-time kicked map. (For an energy-conserving system, varying the strength of a weak magnetic field and thus sweeping through different values of the phase ϕ would produce the same result.) Again, because the perturbation induced by opening up the system is small, there is little mixing among states of different energy. Thus the total probability to remain is obtained simply by averaging the probabilities at the different energies. From Eq. (15) we see that at short times, the classical behavior is recovered:

$$P_{\rm rem} = 1 - \langle S_{\rm lin} \rangle \Gamma t/N = 1 - \Gamma_{\rm cl} t, \tag{19}$$

as $\langle S_{\rm lin} \rangle = A_{\rm lin}(0) = \langle a|a \rangle = 1$ by normalization. Thus at short times, $t \ll \Gamma_{\rm cl}^{-1}$, the faster-decaying scarred states and slower-decaying antiscarred states always cancel exactly and no quantum signature of the underlying classical dynamics can be observed. On the other hand, at long times, i.e., for $t \gg [S_{\rm lin}(E_{\rm min})\Gamma_{\rm cl}]^{-1}$, we obtain the very different behavior

$$P_{\rm rem}(t) = \frac{\langle S_{\rm lin}^{-1} \rangle}{\Gamma_{\rm cl} t}. \tag{20}$$

Here $E_{\rm min}$ is the energy at which the smoothed spectrum has its minimum; for an optimally placed lead $|a\rangle$ this energy is exactly π out of phase with the EBK energy ϕ, as discussed above [Eq. 18)]. $\langle S_{\rm lin}^{-1} \rangle$ is the inverse of the smoothed density of states at $|a\rangle$, averaged over energy (or weak magnetic field).

As $\langle S_{\rm lin} \rangle = 1$ by definition, any fluctuations in the smoothed spectrum resulting from short-time recurrences will cause $\langle S_{\rm lin}^{-1} \rangle$ to be greater than 1, resulting in an enhanced probability to remain at long times. In particular, for an optimally placed lead [corresponding to Eq. (10)], let us consider the strong scarring regime of small λ. This gives the exponentially large enhancement

$$\langle S_{\rm lin}^{-1} \rangle = \left(\frac{\lambda}{2\pi} \right)^2 e^{\pi^2/2\lambda}. \tag{21}$$

This long-time behavior is completely dominated by the most antiscarred states, i.e., those with energy within $O(\lambda)$ of $E_{\rm min} = \phi + \pi$ [Eq. (18)]. For a nonoptimally placed lead, with moderate nonoptimality parameter Q [see Eq. (11) and discussion following] we find empirically a similar exponential enhancement of the long-time probability to remain

$$\langle S_{\rm lin}^{-1} \rangle = \left(\frac{\lambda}{2\pi} \right)^2 e^{(\pi^2/2 - bQ)/\lambda}, \tag{22}$$

where $b = 1.1$ is a numerical constant.

If the state $|a\rangle$ defining the phase-space location of the opening is centered off of the periodic orbit, but within $\hbar$ of the orbit, one still has fluctuations in the linear density of states and consequently an enhancement in the probability to remain at long times. An analytic form for the linear autocorrelation function in such a case can be found in Ref. [30]. For a circular minimum-uncertainty phase-space opening centered a distance δ away from a periodic orbit with small exponent λ, the energy-averaged value $\langle S_{\rm lin}^{-1} \rangle$ scales as

$$\langle S_{\rm lin}^{-1} \rangle \sim \lambda^2 e^{(\pi^2/2 - d\delta/\sqrt{\hbar})/\lambda}, \tag{23}$$

where d is yet another numerical constant. δ can be a displacement along either the stable or unstable direction away from the orbit. Thus, deviations from RMT behavior are observed in an area scaling as $\hbar$ surrounding the periodic orbit. Maximum enhancement of $\langle S_{\rm lin}^{-1} \rangle$ (i.e., enhancement of order $\lambda^2 e^{\pi^2/2\lambda}$) occurs for $\delta < O(\lambda\sqrt{\hbar})$, corresponding to a phase-space area scaling as $\lambda^2\hbar$ surrounding the orbit. Thus, if we consider the long-time probability to remain in the system *averaged over all possible positions of the lead*, we obtain

$$P_{\rm rem} = \frac{1 + O(\hbar \lambda^4 e^{\pi^2/2\lambda})}{\Gamma_{\rm cl} t}. \tag{24}$$

(The correction to RMT is obtained by multiplying the maximum obtainable enhancement by the size of the phase-space region where such enhancement occurs.) In principle, contributions from all the periodic orbits need to be added, however, if orbits with small λ exist, they will clearly dominate any such sum. The result is that at finite energy, exponentially large (in $1/\lambda$) deviations from RMT are found even in the phase-space averaged analysis. In the $\hbar \to 0$ limit of any given classical system, the RMT behavior is recovered because the chance of a lead being found on the short periodic orbit goes to zero. In Sec. IV B, we present theoretical predictions and numerical data measuring the probability to remain in the system at long times as a function of the location of the opening.

B. Probability density at long times and dependence on initial conditions

Up until now we have been focusing on the distribution of resonance widths and on the *total* probability to remain in the system starting from a *uniform* initial state, all as a function of the location of the lead $|a\rangle$. In other words, while changing the location of the opening, we have always been tracing over the initial and final states of the system. We now proceed to address two related questions, both of which re-

quire us to consider transport properties and wave function intensity correlations within the system.

First, still taking the initial filling to be uniform, and fixing the location of the opening to be on a periodic orbit, it is natural to ask how the long-time probability density remaining in the system distributes itself over phase space. Classically, we expect the remaining probability always to be redistributing itself on a time scale short compared to the decay time, and thus to be uniform except in a very narrow corridor encompassing the unstable orbit. The width of the corridor scales as the size of the opening. In RMT, of course, the remaining probability is also completely uniform except at phase space locations having nonzero overlap with $|a\rangle$. In contrast, we find that in the real quantum system, the remaining probability density is strongly suppressed in a corridor of size $\hbar$ around the orbit, much wider than the size of the lead. Even more interesting is the fact that the probability density can be either relatively enhanced or suppressed along the *other* unstable orbits of the system, depending on the classical actions associated with these orbits.

Before proceeding, we mention a closely related problem, which can be thought of as a time-reversed version of the one stated above. Instead of initially filling the system with a uniform density, we inject probability in some known initial state and look at the probability to remain after a long time as a function of this initial state. This state, which we call $|b\rangle$, should be classically well defined, i.e., it can be a phase-space Gaussian, or a position or momentum state, as discussed above.

The two problems are in general distinct: if H is the non-Hermitian quantum Hamiltonian, the first involves the quantity $\langle b|e^{-iH^\dagger t}e^{iHt}|b\rangle$, while the second measures $\langle b|e^{iH^\dagger t}e^{-iHt}|b\rangle$. However, when Γ is very small (in the regime of nonoverlapping resonances), H is nearly normal ($H^\dagger H \approx HH^\dagger$), the distinction between left and right eigenstates vanishes, and the two quantities both converge to the eigenstate sum

$$P^b_{\rm rem}(t)=\sum_n |\langle b|\Psi_n\rangle|^2 e^{-\Gamma_n t}. \tag{25}$$

For $|b\rangle$ not on the periodic orbit containing the lead $|a\rangle$, the quantity $|\langle b|\Psi_n\rangle|^2$ is independent of $\Gamma_n \sim |\langle a|\Psi_n\rangle|^2$, and follows its own chi-squared distribution with mean scaling as $S^b_{\rm lin}(E)$. Here $S^b_{\rm lin}(E)$ is the Fourier transform of the linearized (short-time) autocorrelation function of the test state $|b\rangle$; it is to be distinguished from $S_{\rm lin}(E)\equiv S^a_{\rm lin}(E)$, the smoothed local density of states *at the lead*. We easily obtain, at energy E,

$$P^b_{\rm rem}=\frac{S^b_{\rm lin}(E)}{1+S^a_{\rm lin}(E)\Gamma t/N}\to \frac{S^b_{\rm lin}(E)}{S^a_{\rm lin}(E)}\frac{1}{\Gamma_{\rm cl} t}. \tag{26}$$

Averaging over E, we obtain the ratio of the remaining probability density at $|b\rangle$ to the average remaining density at long times:

$$\frac{P^b_{\rm rem}}{P_{\rm rem}}=\frac{\langle S^b_{\rm lin}/S^a_{\rm lin}\rangle}{\langle 1/S^a_{\rm lin}\rangle}. \tag{27}$$

We see that this ratio goes to unity if $S^b_{\rm lin}$ has no energy dependence, i.e., if $|b\rangle$ does not lie on a short periodic orbit. (Notice that for a Hamiltonian system, the test state $|b\rangle$ is kept fixed, centered at some energy E_0, while we sweep through resonances at different nearby energies E. The question then is whether the center of the test state $|b\rangle$ is or is not close to a periodic orbit at energy E_0. Of course, one could instead imagine shifting the test state so as always to be centered at energy E, in which case it would be more natural to consider short orbits at energy E. The difference is unimportant as long as $E-E_0$ is small compared to the energy width of the Gaussian $|b\rangle$.) If the position $|a\rangle$ of the lead itself does not lie on a periodic orbit, the remaining density profile will of course be flat over *all* states $|b\rangle$. However, if both $|a\rangle$ and $|b\rangle$ lie on periodic orbits, the probability to be found at $|b\rangle$ can be either suppressed or enhanced, depending on whether the energy envelopes $S^a_{\rm lin}$ and $S^b_{\rm lin}$ are in or out of phase in the energy range being averaged over. For simplicity, let us consider an example where the periods and instability exponents of the two orbits are equal. Then the two smoothed energy envelopes are identical, up to a relative phase shift (the difference between ϕ_a and ϕ_b), which can be adjusted by varying a magnetic flux enclosed by one of the orbits. If the two are exactly in phase, $S^a_{\rm lin}=S^b_{\rm lin}$, then the ratio in Eq. (27) reduces to $1/\langle S^{-1}_{\rm lin}\rangle$, which, we recall from our previous discussion, is a quantity exponentially small in the instability exponent λ. Thus, the remaining probability very strongly avoids the orbit on which $|b\rangle$ is located. Another way of expressing this result is that the total probability to remain in the system at long times is exponentially suppressed if the initial state is located on an orbit which is ''in phase'' with the orbit on which the opening is located.

The suppression of probability density given by Eq. (27) is of course a pure quantum interference phenomenon; it has no analog in the classical dynamics of open systems. It is also fundamentally a long-time effect as there is in general no short path leading from $|a\rangle$ to $|b\rangle$ which could give rise to such intensity correlations. However, despite being intrinsically long-time and quantum, the phenomenon can be understood only in terms of the *short-time, classical* dynamics near each of the two unstable periodic orbits. This demonstrates once again the power of semiclassical techniques for understanding long-time quantum behavior.

In the opposite extreme case, where the two orbits are out of phase exactly by $\pi[S^b_{\rm lin}(E)=S^a_{\rm lin}(E+\pi)]$, the ratio in Eq. (27) is dominated by the region of the envelope where $S^b_{\rm lin}$ is maximized and $S^a_{\rm lin}$ minimized. (This is an energy region in which the wave functions tend to be scarred near $|b\rangle$ and antiscarred near $|a\rangle$.) The relative intensity enhancement at $|b\rangle$ then scales with the height of the peak in $S^b_{\rm lin}$, i.e., as $\lambda^{-1}\gg 1$. So a large enhancement of the remaining probability is found on orbits out of phase with the one on which the opening is located.

We need to consider also the case where states $|a\rangle$ and $|b\rangle$ are found on the same orbit (the same reasoning applies if $|a\rangle$ and $|b\rangle$ are on distinct orbits that are related by a symmetry transformation). This corresponds to measuring the remaining probability along the orbit on which the lead is located (or alternatively to launching the initial probability along this orbit). First, consider the case where $|a\rangle$ and $|b\rangle$

are exactly related by time evolution in the closed system. Then the two local densities of states are identical, i.e., $|\langle a|\Psi_n\rangle|^2=|\langle b|\Psi_n\rangle|^2$ for each n. It is easy to see from Eq. (25) that $P_{\rm rem}$ in this case decays at long times as $1/t^2$ instead of the usual $1/t$ behavior. This is easy to understand intuitively: the very long-lived resonances which survive at long times have very little amplitude at $|b\rangle$. More generally, let us consider $|a\rangle$ and $|b\rangle$ lying on the same orbit but not exact time-iterates of one another. This is possible even if $|a\rangle$ and $|b\rangle$ are both optimal [in the sense of having $Q=0$, see Eq. (11)]. Thus, the iterates of $|a\rangle$ may have width $\sigma_0 e^{\lambda n}$ along the unstable manifold as they pass through that point on the orbit on which $|b\rangle$ is centered [31]. If we choose a width for $|b\rangle$ which does not correspond to any integer n, then $|b\rangle$ is not any exact time iterate of $|a\rangle$. However, for some time t we may still write

$$|b\rangle=\alpha|a(t)\rangle+\gamma|c\rangle, \tag{28}$$

where $|\alpha|^2+|\gamma|^2=1$. Then the local density of states at $|b\rangle$ separates naturally into two parts: one of weight $|\alpha|^2$ which is exactly equal to the density of states at the opening $|a\rangle$, and another of weight $1-|\alpha|^2$ which is statistically independent of the former but has the same linear energy envelope. The first, as we just saw, gives a contribution to $P^b_{\rm rem}$ which scales as $1/t^2$ and thus can be ignored at long times. The second behaves just as if $|b\rangle$ were located on a different orbit having the same linear envelope. Thus for $|a\rangle$ and $|b\rangle$ on the same orbit we obtain the same exponential suppression factor as before [Eq. (27)], times the extra suppression factor $1-|\alpha|^2$. This latter factor also becomes very small for small λ [31], as any wave packet optimally placed on a periodic orbit comes ever closer to being an exact time iterate of any other such wave packet on the same orbit.

We note again that this effect is purely quantum mechanical, based though it is on short-time semiclassical analysis. Classically, only a tiny fraction of the probability distribution corresponding to $|b\rangle$ would leak out through the hole at $|a\rangle$ before the density escapes from the periodic orbit and proceeds to distribute itself evenly over the entire accessible phase space.

IV. NUMERICAL TESTS

A. The model

We now proceed to test numerically the various results obtained analytically in the previous section. What is required is a large ensemble of chaotic systems with each realization having a short unstable periodic orbit of the same instability exponent. For this purpose we consider kicked maps on the toroidal phase space $(q,p)\in[-1/2,1/2]\times[-1/2,1/2]$. The classical dynamics for one time step is given by

$$\begin{aligned} p\rightarrow\tilde{p}&=p+mq-V'(q) \mod 1,\\ q\rightarrow\tilde{q}&=q+n\tilde{p}+T'(\tilde{p}) \mod 1. \end{aligned} \tag{29}$$

This dynamics can be obtained from the stroboscopic discretization of a kicked system [32] with a kick potential $-\frac{1}{2}mq^2+V(q)$ applied once every time step and a free evolution governed by the kinetic term $\frac{1}{2}np^2+T(p)$. m and n are arbitrary integers, while V,T are periodic functions of position and momentum, respectively. The system can also be thought of as a perturbation of the linear system (cat map) [33]

$$\begin{aligned} p\rightarrow\tilde{p}&=p+mq \mod 1,\\ q\rightarrow\tilde{q}&=np+(mn+1)q \mod 1. \end{aligned} \tag{30}$$

For given positive integers m,n, we choose the functions V and T such that $m-V''(q)>0$ for all q and similarly $n+T''(\tilde{p})>0$ for all $\tilde{p}$. Then the system is strictly chaotic and looks everywhere locally similar to an inverted harmonic oscillator.

The quantization of such systems is well-studied in the literature [32]. $\hbar$ must be chosen such that $N=1/2\pi\hbar$, the number of h-sized cells in the classical phase space, is an integer (N must be even to preserve the periodicity of the quadratic terms in the potential and kinetic energy). For doubly periodic boundary conditions, the quantum N-dimensional Hilbert space is spanned by the position basis $|q_i\rangle$, where $q_i=i/N$ and $i=0,\ldots,N-1$. The momentum-space basis is given similarly by $|p_j\rangle$, where $p_j=j/N$ and $j=0,\ldots,N-1$; and the two bases are related by a discrete Fourier transform. The quantum dynamics is then given by a unitary $N\times N$ matrix

$$\begin{aligned} U=&\exp\left[-i\left(\frac{1}{2}n\hat{p}^2+T(\hat{p})\right)\Big/\hbar\right]\\ &\times\exp\left[i\left(\frac{1}{2}m\hat{q}^2-V(\hat{q})\right)\Big/\hbar\right]. \end{aligned} \tag{31}$$

Each factor is evaluated in the appropriate basis, and an implicit forward and backward Fourier transform has been performed.

We may now perturb this unitary dynamics to allow for a small decay rate in channel a:

$$W=\left(1-\frac{\Gamma}{2}|a\rangle\langle a|\right)U. \tag{32}$$

Equation (32) is of course the discrete-time version of the continuous-time dynamics given in Eq. 2 above. Since we are working in the regime $\Gamma\ll 1$, where the decay rate per time step is small, the discretization of the decay process will not affect the long-time behavior of the system. The decay channel $|a\rangle$ can in principle represent any vector in the Hilbert space; however, for the decay to correspond to a classical escape route, $|a\rangle$ should be a phase-space localized state, such as a position or momentum state. We will find it convenient to let $|a\rangle$ be a circular phase-space Gaussian in the coordinates q,p.

We now need to construct an ensemble of such systems, all having the same behavior in the vicinity of a short unstable periodic orbit. For this purpose, we set $m=n=1$, and let the potential V and kinetic term T be odd functions of their respective arguments

$$V(q)=\sum_{r=1}^{3}\left[K_r\sin(2\pi rq)-2\pi K_r rq\right], \tag{33}$$

$$T(p)=\sum_{r=1}^{3}\left[K_r'\sin(2\pi rp)-2\pi K_r' rp\right]. \tag{34}$$

It is easy to see that the equations of motion [Eq. (29)] then have a fixed point at the origin with Jacobian matrix

$$J=\begin{bmatrix}1 & 1\\ 1 & 2\end{bmatrix}$$

[the system can be thought of as a perturbation of the

$$\begin{bmatrix}1 & 1\\ 1 & 2\end{bmatrix}$$

cat map, with perturbation vanishing near $(q,p)=(0,0)$]. The instability exponent is given by $\lambda=\cosh^{-1}(\frac{1}{2}\mathrm{Tr}J)=0.96$. We may now choose each of the coefficients K_r, K_r' from a uniform distribution over the interval $[-0.3/(2\pi r)^2, 0.3/(2\pi r)^2]$. One easily sees that each system in this ensemble satisfies everywhere the condition $1-V''>0$, $1+T''>0$ mentioned above, which is sufficient to ensure hard chaos.

B. Probability to remain

The ensemble-averaged probability to remain in the system after t time steps is now computed for various positions of the exit channel $|a\rangle$. For simplicity, we choose $|a\rangle$ to be a circular phase-space Gaussian

$$a(q)\sim e^{-(q-q_0)^2/2\hbar+ip_0(q-q_0)/\hbar} \tag{35}$$

centered on (q_0,p_0) and having width $\sqrt{\hbar}$ in both the q and p directions. Because the Jacobian J at the fixed point $(0,0)$ is symmetric (and the stable and unstable directions are thus locally orthogonal), such a wave packet, when centered at $(0,0)$, is optimal in the sense of having the slowly decaying short-time autocorrelation function of Eq. (10). (A more general Gaussian wave packet (including position or momentum states as extreme limits) centered on the periodic orbit may have a nonzero parameter Q [see Eq. (11)], leading to a less sharp linear spectral envelope and less strong scarring and antiscarring effects. The qualitative behavior would, however, remain unchanged.)

In Fig. 2, the probability to remain in the system as a function of the scaled time $t'=\Gamma_{\mathrm{cl}}t$ is first plotted (using plusses) for a generic leak location. The data was collected for systems of size $N=120$ and decay parameter $\Gamma=0.1$. The results agree well with the the RMT prediction $P_{\mathrm{rem}}(t')=1/(1+t')$ (dashed curve). For comparison, the classical probability to remain, $\exp(-t')$, is plotted as a dotted curve. Next, we place the opening on the periodic orbit at the origin of phase space, and obtain the rather different behavior, with an enhanced long-time tail (squares). The asymptotic form is well reproduced by the scar theory prediction $P_{\mathrm{rem}}(t')\approx\langle S_{\mathrm{lin}}^{-1}\rangle/t'$, which is shown in Fig. 2 as a solid line. For the instability exponent $\lambda=0.96$, we observe a long-time probability enhancement factor $\langle S_{\mathrm{lin}}^{-1}\rangle=11.04$. Of course, bigger enhancement factors can be observed for less unstable orbits, as we will see below.

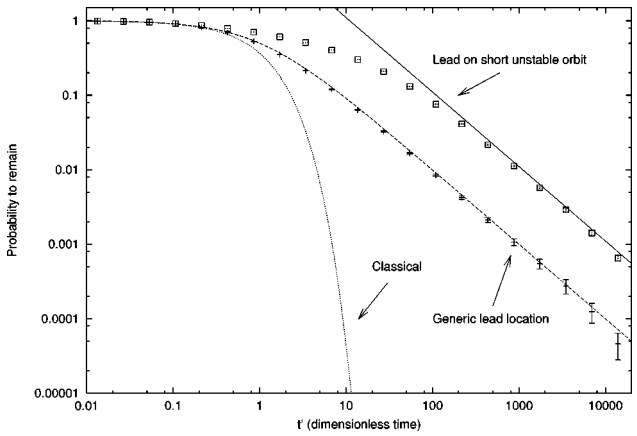

FIG. 2. The probability to remain in the open quantum system is plotted as a function of scaled time $t'=\Gamma_{\mathrm{cl}}t$. The classical prediction $\exp(-t')$ is shown as a dotted curve. The quantum probability to remain for a generic lead location (pluses) compares well with the RMT prediction $1/(1+t')$ (dashed curve). For a lead placed on a short periodic orbit with instability exponent $\lambda=0.96$, we obtain the enhanced long-time probability to remain (squares), which agrees with the scar theory prediction $\langle S_{\mathrm{lin}}^{-1}\rangle/t'$ (solid line). The system size used for obtaining the data is $N=120$ and the decay rate per step in the exit channel is $\Gamma=0.1$.

First, we examine more carefully the probability to remain at long times as a function of the position of the lead. In Fig. 3(a) is plotted the total probability to remain in the system at time $t'=2\times10^3$, for various locations of the opening (all for $N=30$). These possible locations are located on a 40×40 grid filling the middle 1/9 th section of the total phase space (i.e., $(q,p)\in[-1/6,1/6]\times[-1/6,1/6]$). The bright spot at the center of the figure represents the enhanced probability to remain if the opening is located exactly on the periodic orbit. As we see from the figure, the antiscarring effect falls off quite quickly as the opening is moved away from the periodic orbit [in fact, the size of the bright spot scales as $\hbar$; see Eq. (23) and discussion following]. In Fig. 3(b) is plotted the theoretical quantity $\langle S_{\mathrm{lin}}^{-1}\rangle$, as computed using the linearized equations of motion [Eq. (30)] around the periodic orbit. This is observed to be in good agreement with the data. Of course the linearized equations of motion only hold near the periodic orbit itself, and do not correctly describe classical motion in other regions of phase space. However, in our case the short periodic orbit at the origin clearly dominates the data. If the classical system contained several not very unstable orbits (see next subsection for an example), several bright spots would appear in the plot, and each could then be well reproduced using the linearized classical dynamics around the appropriate orbit.

An important feature to notice in Fig. 3 is that $P_{\mathrm{rem}}(t)$ at long times depends not only on the distance of the lead from the periodic orbit but also on the direction. Greater enhancement is observed if the lead is placed along either the stable or the unstable manifold of the orbit (the two ''diagonals'' of the would-be ''square'').

We now consider how the probability to remain at long times depends on the instability exponent λ of the orbit on

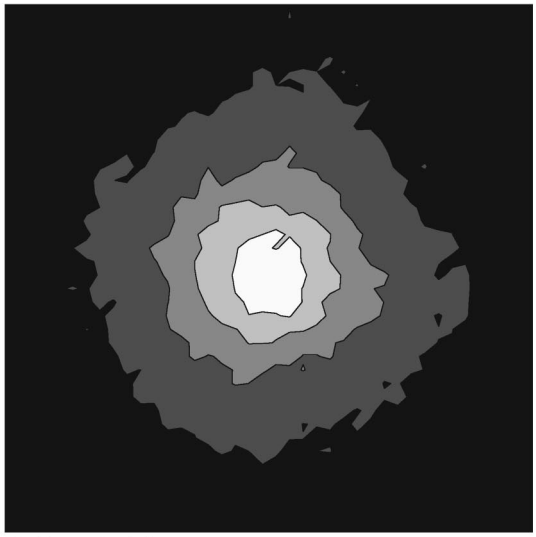

(a) *Numerical data*

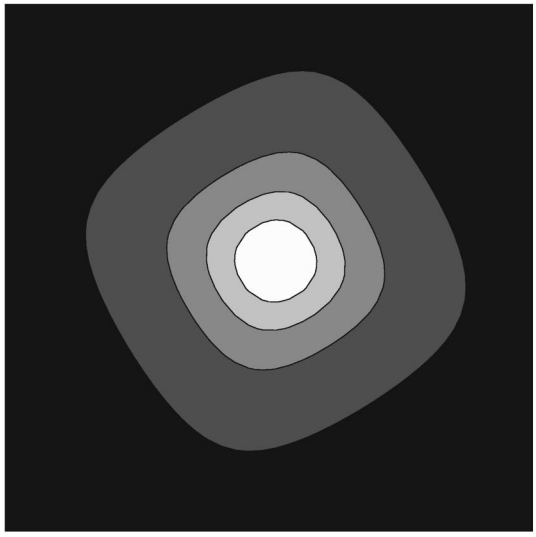

(b) *Scar theory prediction*

FIG. 3. The remaining probability density after time $t'=2\times10^{-3}$, as a function of the position of the lead. In (a), the numerical data is presented for an ensemble of systems of size $N=30$; in (b) we show the theoretical prediction $\langle S_{\rm lin}^{-1}\rangle/t'$. At the center of each plot is an unstable periodic orbit of exponent $\lambda=0.96$: for a lead placed at that position (white spot) the probability at long times is enhanced by a factor of 11 over the same probability for a generic lead position (black background). Notice the anisotropy: more enhancement at long times is predicted (and observed) when the displacement of the lead away from the periodic orbit is along one of the invariant manifolds.

which the lead is located. As we discussed in the previous section, as λ gets small, resonances exponentially narrow in λ should appear at the antiscarring energies, and the total probability to remain at long times is enhanced by a factor exponentially large in λ [Eq. (21)]. To see this effect, we modify the classical dynamics of Eq. (29) by adding an additional term to the potential and kinetic functions:

$$V(q)=\cdots-\frac{\Delta}{(2\pi)^2}\cos(2\pi q),$$

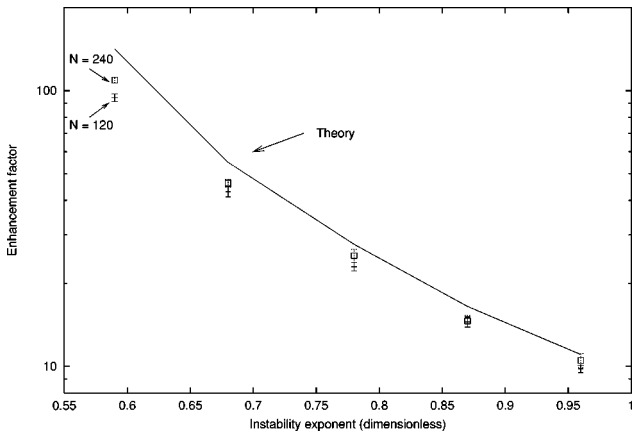

FIG. 4. The long-time enhancement factor of the probability to remain in a system when the lead is placed on a periodic orbit is plotted as a function of the instability exponent of the orbit. Data are shown for $N=120$ (pluses) and $N=240$ (squares). The $N\to\infty$ theoretical prediction $\langle S_{\rm lin}^{-1}\rangle$ is shown as a solid curve. We see the exponential increase in the probability to remain as the exponent λ decreases [the $\lambda\to0$ asymptotic form is given in Eq. (21)]. For large λ, the enhancement factor converges to 1, the RMT prediction.

$$T(p)=\cdots+\frac{\Delta}{(2\pi)^2}\cos(2\pi p). \tag{36}$$

The same value of Δ should be used in the potential and kinetic terms to preserve the symmetry of the Jacobian. The Jacobian matrix of the dynamics near the periodic orbit at (0,0) is then given by

$$\begin{bmatrix} 1 & 1-\Delta \\ 1-\Delta & 1+(1-\Delta)^2 \end{bmatrix}. \tag{37}$$

For positive Δ, the trace of the Jacobian decreases and the orbit becomes less unstable. Using $\Delta=0.0$, 0.1, 0.2, 0.3, and 0.4, we obtain exponents 0.96, 0.87, 0.78, 0.68, and 0.59, respectively.

In Fig. 4 the long-time enhancement factor of $P_{\rm rem}(t)$ over its RMT value is plotted as a function of the exponent λ, using plusses for $N=120$ and squares for $N=240$. The theoretical prediction $\langle S_{\rm lin}^{-1}\rangle$ is shown as a solid curve. The data consistently falls below the theoretical prediction, with the disagreement becoming more pronounced at the smaller values of λ. The reason is primarily a finite-size effect: the analytical calculations are all carried out under the assumption that the mean level spacing is much smaller than any scale over which the linear energy envelope changes significantly. Then the linear envelope is roughly constant on the scale at which individual resonances emerge, and their behavior can be treated statistically. Thus, the discrepancy becomes more noticeable as $\lambda\to0$ for fixed N, as the structures in $S_{\rm lin}$ become more comparable to the mean level spacing. Indeed, we see that the $N=240$ data is consistently closer than the $N=120$ data to the theory, which strictly applies only in the semiclassical $N\to\infty$ limit.

We observe the exponential increase in the enhancement factor as λ decreases; indeed the very moderate exponent $\lambda=0.59$ produces an enhancement factor of well over 100 in

the long-time probability to remain. $\lambda = 0.1$ would in theory produce an average long-time enhancement of 1.2×10^{13}, provided we were able to go to a large enough system, wait for a long enough time, and collect enough statistics to observe it [from Eq. (15) we see that the asymptotic $1/S_{\rm lin} t'$ form holds only for $t' \gg S_{\rm lin}^{-1}$].

C. Phase space distribution of long-time probability density

We now consider predictions concerning the enhancement or suppression of the long-time probability near orbits *other* than the one on which the lead is located (see discussion in Sec. III B). To test these predictions we need an ensemble of systems all having two periodic orbits in common, and the ability to vary the action phase difference between them. In our example the two orbits have the same local dynamics in their respective neighborhoods, though this of course is not necessary to produce the desired effect.

We work on the phase space $(q,p) \in [-1/4,3/4] \times [-1/2,1/2]$, set $m=n=2$ in the equations of motion [Eq. (29)], and impose the constraint $K_1 = -3K_3$ on the kick potential [see Eq. (33)]. This condition ensures the presence of a fixed point at $(1/2,0)$ in addition to the usual one at $(0,0)$ on which we have been focusing so far. The linearized dynamics around each orbit is given by the Jacobian

$$J = \begin{bmatrix} 1 & 2 \\ 2 & 5 \end{bmatrix},$$

and the exponent per period is $\lambda = 1.76$. Other orbits are of course present, but they change with the coefficients K_r, K_r', and so their effects are expected to cancel out in the process of ensemble averaging. In order for the two orbits not to be related by a symmetry transformation we only need all the K_r to be nonvanishing.

Our analysis showed that the behavior of the remaining probability density at long times should depend strongly on the relative action phase difference between the two orbits. This phase difference can be easily controlled by adjusting K_2 ($\phi_b - \phi_a = NK_2/4$). Fixing K_2 at a nonzero value which produces $\phi_b - \phi_a = 0 (\mathrm{mod}\, 2\pi)$, we are free to vary K_3 and the three coefficients K_r' consistent with the constraints $2 - V'' > 0$ and $2 + T'' > 0$ (which are sufficient to ensure hard chaos). We obtain then, for $N=80$ and $\Gamma = 0.1$, the results shown in Fig. 5(a). Clearly the remaining probability is very strongly suppressed on the orbit on the left, where the lead is located (as we saw in the previous section, the probability to remain *exactly* on the orbit falls off faster with time than probability elsewhere, so the numerical value of the relative suppression there will be time dependent). We also see mild density suppression on the two orthogonal invariant manifolds of this orbit. The phenomenon we want to focus on, though, is the suppression we observe on the orbit on the right side of Fig. 5(a). The observed suppression factor right on the periodic orbit at $(1/2,0)$ is 0.37, compared with the predicted value 0.45; again the discrepancy may possibly be attributed to finite size effects. As expected, we also observe probability suppression along the manifolds of this second orbit.

We now consider the opposite case, where the two orbits are exactly out of phase [$\phi_b - \phi_a = \pi (\mathrm{mod}\, 2\pi)$]. Adjusting

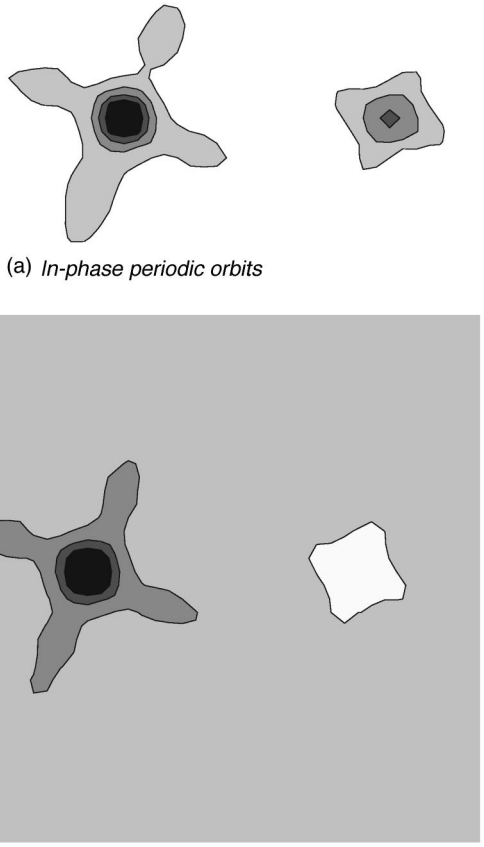

(a) *In-phase periodic orbits*

(b) *Out-of-phase periodic orbits*

FIG. 5. The remaining probability distribution at very long times is shown for an ensemble of systems (of size $N=80$) all having two short periodic orbits in common, each with instability exponent $\lambda = 1.76$. In both cases, the lead is centered on the periodic orbit on the left side of the plot. The remaining probability is strongly suppressed on that orbit and less so on its invariant manifolds. The action of the orbit on the right is chosen to be in phase with the first one in case (a), so that probability there is also suppressed, and exactly out of phase with it in case (b), leading to an enhancement of the probability density on the second orbit and its invariant manifolds. See next figure for quantitative comparison with the theory.

K_2 appropriately, we again perform ensemble averaging over the other parameters and obtain the results in Fig. 5(b). The same suppression is still seen along the orbit containing the lead and its invariant manifolds. However, we now see, as expected, an *enhancement* of the remaining probability density near the orbit on the right. The enhancement factor on that orbit itself is 1.78; the theoretical prediction is 1.67.

The predicted relative intensity at the orbit $(1/2,0)$ [Eq. (27)] given a lead at $(0,0)$ is plotted in Fig. 6 as a function of the action phase difference between the two orbits. (One could imagine obtaining such a plot in a physical system by tuning a weak magnetic field which had little effect on the classical dynamics but did change the relative phase between two orbits enclosing different amounts of flux. Alternatively, if the periods of the two orbits differed, the orbits could be observed to go in and out of phase with one another as one changed the energy range in which the resonances were populated.) The suppression and enhancement factors in this case never get very far from unity, due to the relatively large

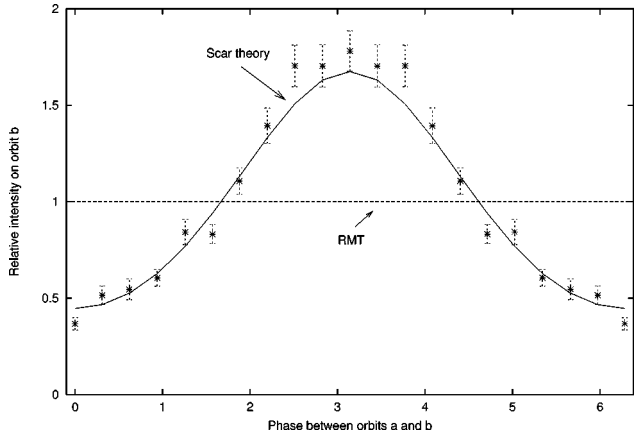

FIG. 6. The predicted relative intensity at long times on a periodic orbit other than the one containing the lead is plotted as a function of the relative phase between the two orbits (solid curve). For reference, the phase-space averaged intensity is plotted as a dashed line. Intensity suppression is predicted and observed when the orbits are in phase, and enhancement is seen when the orbits are exactly out of phase [compare (a) and (b) in previous figure]. The data are collected for an ensemble of systems with $N=80$, and each orbit has instability exponent $\lambda=1.76$.

value of the instability exponent λ chosen for our example. Values obtained numerically, as described in the preceding paragraphs, are given for comparison with scar theory, along with statistical error bars. The dashed line at 1 represents the RMT prediction.

V. CONCLUSION

We have concentrated throughout on leakage through a single decay channel which is very well localized in phase space (leak area much less than h). One would like to understand more generally possible scar effects for multichannel leads as well as for leads wide enough to produce overlapping resonances. A detailed treatment of such effects is outside the scope of the present work. However, one possible extension turns out to be relatively straightforward, and the results suggest that the most interesting scar effects are already captured in the single channel analysis. Specifically, consider M decay channels, each with a slow decay rate, as in Eq. (6). If the sum of these classical rates is small compared to the quantum level spacing, the resulting resonances will be nonoverlapping, and a perturbative approach to the problem is valid. In RMT, the probability to remain at long times is given by a product of factors associated with each of the leads [Eq. (8)]. In the case where one of the channels happens to be close to a short periodic orbit, the intensity distribution giving rise to this one factor only will be affected, producing the same overall enhancement factor $\langle S_{\rm lin}^{-1}\rangle$ obtained previously. The total probability $P_{\rm rem}$ now falls off much more quickly with time than in the single-channel case, reflecting the fact that it is much harder to find a resonance which is slowly decaying through *all* of the channels. However, the essential observation of an enhanced probability of finding very narrow resonances survives. Clearly the analysis is more complicated for correlated decay channels, and for the case of larger total decay rates where the resonances become overlapping. Still, periodic orbits by their very nature produce quantum effects in phase space regions of size $\hbar$ surrounding the orbit; thus our intuition tells us that no fundamentally new scar effects are expected in most cases for multichannel leads.

We have seen that an analysis of short time classical motion in a chaotic system can shed much light on quantum behavior on the scale of the decay time, which is much larger than the Heisenberg time and every other time scale in the system. This is somewhat counterintuitive, as the narrow resonance regime is by its very nature nonclassical and is associated with the very long-time behavior of the system. Even though in some cases (e.g., in the presence of strong diffraction or caustics) semiclassical methods may not be sufficient to predict the properties of individual high-energy quantum chaotic wave functions, they are still very powerful for making statistical predictions of the sort described in this paper. We note that a small change in the system potential, or the presence of a few impurity scatterers may completely change the character of individual resonances in an open system, making comparison with exact semiclassical wave functions futile. On the other hand, the scar theory predictions, which concern statistical properties such as the distribution of resonance widths, are robust to such changes in the details of the system, as long as the dynamics of the first few bounces is known. In a situation where the classical dynamics of the quantum system under study is not known reliably even for short times, one could use methods similar to those described here to search for the short unstable periodic orbits. This can be done by moving the position of the lead, or, more practically in many situations, by adjusting some system parameter which changes the classical dynamics of the system. For a given classical system and lead position, one then sweeps through a weak magnetic field or some other parameter not affecting the classical dynamics, and searches for a large fraction of very narrow resonances, occurring periodically in the magnetic field strength.

Clearly the ideas described here can also be extended to study two-lead systems, where properties such as conductance peak height distributions can be analyzed. In analogy with the present work, the results will strongly depend on whether one or both of the leads is located on a short unstable classical orbit. Where the leads are found on two different short periodic orbits, the phase difference between them can be varied to produce an enhancement or suppression of the average conductance, as suggested by the results of the present work. Even stronger effects can be observed if the leads are located on the same periodic orbit, or if the two orbits are related to each other by a symmetry of the system. These issues and other related questions are addressed fully in a forthcoming paper [27]. Certainly much more work needs to be done generally in understanding classical dynamics effects on the quantum properties of open chaotic systems.

ACKNOWLEDGMENTS

This research was supported by the National Science Foundation under Grant No. 66-701-7557-2-30. Initial work on this project was performed during a stay at the Technion in Israel. The author thanks E. J. Heller for many useful conversations.

[1] S. Sridhar, Phys. Rev. Lett. **67**, 785 (1991).
[2] J. Stein and H.-J. Stöckman, Phys. Rev. Lett. **68**, 2867 (1992).
[3] T.M. Fromhold, P.B. Wilkinson, F.W. Sheard, L. Eaves, J. Miao, and G. Edwards, Phys. Rev. Lett. **75**, 1142 (1995); P.B. Wilkinson, T.M. Fromhold, L. Eaves, F.W. Sheard, N. Miura, and T. Takamasu, Nature (London) **380**, 608 (1996).
[4] D. Wintgen and A. Honig, Phys. Rev. Lett. **63**, 1467 (1989).
[5] K. Muller and D. Wintgen, J. Phys. B **27**, 2693 (1994).
[6] E.J. Heller, Phys. Rev. Lett. **53**, 1515 (1984).
[7] E.B. Bogomolny, Physica D **31**, 169 (1988).
[8] M.V. Berry, *Les Houches Lecture Notes, Summer School on Chaos and Quantum Physics*, edited by M-J. Giannoni, A. Voros, and J. Zinn-Justin (Elsevier, Vanconver, Canada 1991); M.V. Berry, Proc. R. Soc. London, Ser. A **243**, 219 (1989).
[9] O. Agam and S. Fishman, Phys. Rev. Lett. **73**, 806 (1994); O. Agam and S. Fishman, J. Phys. A **26**, 2113 (1993).
[10] L. Kaplan and E.J. Heller, Ann. Phys. (N.Y.) **264**, 171 (1998).
[11] T.M. Antonsen, Jr., E. Ott, Q. Chen, and R.N. Oerter, Phys. Rev. E **51**, 111 (1995).
[12] L. Kaplan, Phys. Rev. Lett. **80**, 2582 (1998).
[13] V.I. Fal'ko and K.B. Efetov, Phys. Rev. B **52**, 17 413 (1995); I.E. Smolyarenko and B.L. Altshuler, *ibid.* **55**, 10451 (1997).
[14] A. Lupu-Sax, I.E. Smolyarenko, L. Kaplan, and E.J. Heller (unpublished).
[15] S.M. Cronenwett, S.R. Patel, C.M. Marcus, K. Campman, and A.C. Gossard, Phys. Rev. Lett. **79**, 2312 (1997); J.A. Folk, S.R. Patel, S.F. Godijn, A.G. Huibers, S.M. Cronenwett, C.M. Marcus, K. Campman, and A.C. Gossard, *ibid.* **76**, 1699 (1996); C.M. Marcus, S.R. Patel, A.G. Huibers, S.M. Cronenwett, M. Switkes, I.H. Chan, R.M. Clarke, J.A. Folk, S.F. Godijn, K. Campman, and A.C. Gossard, Chaos Solitons Fractals **8**, 1261 (1997).
[16] P. Gaspard and S.A. Rice, J. Chem. Phys. **90**, 2225 (1989).
[17] B. Eckhardt, Chaos **3**, 613 (1993).
[18] P. Cvitanovic and B. Eckhardt, Phys. Rev. Lett. **63**, 823 (1989).
[19] R. Blumel and U. Smilansky, Phys. Rev. Lett. **60**, 477 (1988); **64**, 241 (1990); Physica D **36**, 111 (1989).
[20] E. Doron, U. Smilansky, and A. Frenkel, Physica D **50**, 367 (1991).
[21] R.A. Jalabert, H.U. Baranger, and A.D. Stone, Phys. Rev. Lett. **65**, 2442 (1990).
[22] C. Jung and T.H. Seligman, J. Phys. A **28**, 1507 (1995); Phys. Rep. **285**, 77 (1997); C. Jung, C. Mejia-Monasterio, and T.H. Seligman, Phys. Lett. A **198**, 306 (1995).
[23] F. Borgonovi, I. Guarneri, and D. Shepelyansky, Phys. Rev. A **43**, 4517 (1991); F. Borgonovi and I. Guarneri, J. Phys. A **25**, 3239 (1992); Phys. Rev. E **48**, R2347 (1993); F. Borgonovi, I. Guarneri, and L. Rebuzzini, Phys. Rev. Lett. **72**, 1463 (1994).
[24] B.L. Altshuler, V.E. Kravtsov, and I.V. Lerner, JETP Lett. **45**, 199 (1987); B.A. Muzykantskii and D.E. Khmelnitskii, Phys. Rev. B **51**, 5480 (1995); A.D. Mirlin, JETP Lett. **62**, 603 (1995).
[25] G. Casati, G. Maspero, and D.L. Shepelyansky, Phys. Rev. E **56**, R6233 (1997); K.M. Frahm, *ibid.* **56**, R6237 (1997); D.V. Savin and V.V. Sokolov, *ibid.* **56**, R4911 (1997); Y.V. Fyodorov, D.V. Savin, and H.-J. Sommers, *ibid.* **55**, R4857 (1997); F.-M. Dittes, H.L. Harney, and A. Müller, Phys. Rev. A **45**, 701 (1992); H.L. Harney and F.-M. Dittes, Ann. Phys. (N.Y.) **220**, 159 (1992).
[26] D.L. Miller, e-print cond-mat/9801245.
[27] W.E. Bies, L. Kaplan, and E.J. Heller (unpublished).
[28] J.U. Nockel and A.D. Stone, Nature (London) **385**, 45 (1997); J.U. Nockel, A.D. Stone, G. Chen, H.L. Grossman, and R.K. Chang, Opt. Lett. **21**, 1609 (1996).
[29] S.C. Creagh and N.D. Whelan, e-print chao-dyn/9808014 (unpublished); S.C. Creagh and N.D. Whelan, Phys. Rev. Lett. **77**, 4975 (1996).
[30] P.W. O'Connor, S. Tomsovic, and E.J. Heller, Physica D **55**, 340 (1992).
[31] L. Kaplan and E. J. Heller, Phys. Rev. E (to be published).
[32] G. Casati, B.V. Chirikov, F.M. Izrailev, and J. Ford, in *Stochastic Behavior in Classical and Quantum Hamiltonian Systems*, edited by G. Casati and J. Ford (Springer, New York, 1979); M.V. Berry, N.L. Balazs, M. Tabor, and A. Voros, Ann. Phys. (N.Y.) **122**, 26 (1979).
[33] P.A. Boasman and J.P. Keating, Proc. R. Soc. London, Ser. A **449**, 629 (1995).